Highly dispersive waterborne polyurethane/ZnO nanocomposites for corrosion protection

**Gnanaprakasam Christopher, Manickam Anbu Kulandainathan,
Gurusamy Harichandran**

Abstract The interfacial interactions between surface-modified zinc oxide with oleic acid (OA-ZnO) and polymer matrix have important effects on the properties of nanocomposites. This zinc oxide nanoparticle was synthesized and characterized by various techniques such as field emission scanning electron microscopy, X-ray diffraction, and Fourier transform infrared spectroscopy. The water contact angle of waterborne polyurethane (WPU) nanocomposites is found to be increased with the addition of OA-ZnO compared with pure WPU. The corrosion protection of the polyurethane nanocomposites coatings on mild steel was assessed by potentiodynamic polarization and electrochemical impedance spectroscopy techniques. Coating with OA-ZnO in the WPU matrix showed the enhancement of resistance of mild steel to corrosion. This can be related to the surface modification by oleic acid which enhances the dispersion of nano-ZnO and improves the corrosion resistance of the WPU coating. Compared with unmodified ZnO nanoparticles, there were noticeable improvements in the hydrophobicity, corrosion protection, and uniform dispersion without agglomeration, and also improvement in the antisettling behavior when surface-modified ZnO nanoparticles with oleic acid (OA-ZnO) were used.

Keywords Nanoparticles, Corrosion, Waterborne polyurethane, Nano-ZnO

G. Christopher, G. Harichandran (✉)
Department of Polymer Science, University of Madras,
Guindy Campus, Chennai 600 025, India
e-mail: umghari@gmail.com

M. Anbu Kulandainathan
Electro-organic Division, Central Electrochemical Research
Institute, Karaikudi 630006, India

Introduction

Protecting metals from corrosion is being looked upon as a process that needs frequent updates. Nanoparticles have gained prominence in working against corrosion—results of various research are proof of their active involvement in improving the resistance of metals to corrosion. Corrosion is an electrochemical phenomenon, occurring at the metal–solution interface, where the metal is oxidized and oxygen reduced from the solution. The interactions of metals with their corrosive environment through electrochemical reactions lead to degradation and deterioration of metals, causing huge loss of energy and economy worldwide. To prevent this degradation, the surface of metal should be protected.[1–4] Steel is a common metal used in different structures, due to its good physical and mechanical properties, but its electrochemical nature can easily corrode. There are three major approaches used to protect metals from aggressive environments: corrosion inhibitors, cathodic protection, and barrier protection. The barrier protection method is mostly used in the paints and coating industry to isolate the metal substrate from the corrosive environment.[5–9]

Organic coatings are the best barrier protection method, which protect metals against corrosive species. The advantage of these coatings is that they contain binders, conventional pigments, or fillers. The incorporation of such materials in the coatings could improve many properties such as UV resistance, corrosion resistance, mechanical properties (scratch and abrasion resistance), etc. But these conventional pigments at high dosages have a few disadvantages, such as the loss of impact resistance, optical properties, poor adhesion, reduced coating flexibility, inferior abrasion and scratch resistance, early delamination, and an increase in coating viscosity. To avoid these problems, incorporation of nanosized pigments and

fillers in the coatings is a modern approach leading to improvement in the performance of the coatings even at low concentrations. Furthermore, nanofillers have better barrier properties in coatings than micron-sized fillers.[4–7]

Numerous kinds of polymers have been used as binders for barrier coatings to prevent metals from corrosion. The recent environmental regulations and acts have been imposed on paints and coatings industries to use ecofriendly metals in polymeric coatings to avoid health hazards and toxicity problems.[4,8,9] To meet this requirement, the volatile organic compounds (VOCs) in polymeric coatings have been reduced by using modern coatings technologies such as vegetable oil-based polymeric coatings, waterborne polymeric coatings, UV curable coatings, and high solids coatings. Among these coatings, polyurethane dispersion coating uses a unique waterborne polymer, a binary colloidal system, which can be applied as a potential alternative for solventborne coatings.

The advantages of waterborne polyurethanes (WPUs) are ecofriendliness, low viscosity, easy cleaning, nontoxicity, and good applicability. However, they have some drawbacks, such as weak water resistance and weak thermal and mechanical properties in the coatings. Improvements in mechanical, rheological, anticorrosive, and light-resistance properties of WPU matrices incorporated with nanometal oxides such as TiO_2, Fe_2O_3, ZnO, SiO_2, Al_2O_3, $CaCO_3$, and zirconia have been studied for more than two decades.[10–14]

The property enhancement of barrier coatings is strongly connected with the interfacial interactions between the polymer and the dispersion degree of the nanoparticles. There are many emerging applications where it is necessary to disperse nanoparticles into a polymer matrix.[15–19] These dispersed particle systems are mainly used to enhance or improve the properties of the composite material, such as conductivity, strength, energetics, corrosion resistance, optical properties, and so on. One of the main reasons for using nanoparticles is their large surface-to-volume ratio which increases the number of particle–matrix interactions, thus increasing the effects on the overall material properties. Proper dispersion of nanoparticles into the polymer matrix can be achieved through either chemical or electrochemical treatment where modifying agents, such as silane, polyacrylicacid, polystyrene, polymethylmethacrylate, long-chain fatty acids (stearic acid, oleic acid, etc.), silane coupling agents, alkanoic acids, etc., are employed to modify the surface of the nanoparticles.[20–29] Among these surface modifiers, oleic acid has gained more attention recently, owing to its hydrophobic nature. The nanoparticle surfaces of SiO_2, ZnO, Fe_2O_3, $CaCO_3$, alumina, etc., coated with oleic acid have been reported earlier.[30–38] Although a few references are available for WPU coatings involving nanoparticles of metal oxides coated with oleic acid, anticorrosive behavior of a WPU coating with oleic acid as a surface-modifying agent for ZnO has not been reported so far.

In the present study, novel WPU nanocomposites are prepared using a solution-blending technique, where various dosages (0.1%, 0.2%, and 0.3%) of OA-ZnO are incorporated into the WPU matrix. The resultant nanocomposites are coated on mild steel (MS) and studied for their resistance to corrosion using potentiodynamic polarization and electrochemical impedance spectroscopy (EIS).

Materials and methods

Raw materials

WPU dispersion (PU-687) was procured from Piccassian Polymers and analar grades of oleic acid, dichloromethane, zinc acetate, sodium hydroxide, and methanol were from S. D. Fine Chemicals (Mumbai, India).

Synthesis of nano-ZnO and surface-modified nano-ZnO

Unmodified and modified nano-ZnO were synthesized using a reported method with minor modifications as explained below. A solution of zinc acetate (1.0 M) was added dropwise into a solution of sodium hydroxide (2 M) and mixed vigorously at a temperature of about 55°C for 40 min. The resultant white precipitate of ZnO was washed with deionized water and ethanol and dried at 60°C. The dried particles were then subjected to calcination at 400°C for 3 h.[39]

Preparation of surface-modified ZnO nanoparticles

Oleic acid (0.02 mmol) was added to a suspension containing 5 mg of the prepared ZnO nanoparticles in 2 mL of dichloromethane. The mixture was then stirred at room temperature for 1 h. The solid residue obtained after solvent evaporation was collected and washed with excess methanol and dried.[36]

Preparation of nanocomposite coatings

Experiments were conducted by dispersing various dosages (0.1%, 0.2%, and 0.3% (w/w)) of the OA-ZnO nanoparticles into a WPU matrix by solution-blending method and ultrasonification. Bare MS (composition of MS is 0.045% P, 0.3% Si, Cr, N, Cu, 0.3–0.65% Mn, 0.05% S, 0.14–0.28% C, and the remainder is Fe) panels were dipped into the resulting nanocomposites and dried at 75°C for 30 min. After maintaining for 72 h at room temperature, the panels were subjected to electrochemical studies. Before coating, mild steel was cleaned with acetone, ethanol, and double-distilled water to make the surface free from dust particles, oils,

and surface oxides. The thickness of the coating was in the range of 15–20 μm. Synthesis of the nanocomposites and the subsequent steps that followed (right from dispersion of the nanocomposites into the polymer to the corrosion resistance tests) were repeated thrice to confirm the consistency of the obtained results.

Characterization methods

Surface structures of all samples were characterized using a Model Y 40 (of Perkin-Elmer, USA) Fourier transform-infrared (FTIR) spectroscope. Measurements were carried out with pressed pellets made from KBr powder. The FTIR spectrum was measured between the wave number of 400 and 4000 cm^{-1}. The bare and the modified ZnO nanoparticles were characterized using a Brucker D8 advance diffractometer. The diffractometer involved monochromatic Cu $K\alpha_1$ radiation (λ = 1.5418 Å), with a voltage of 40 kV and a current of 20 mA. Studies based on field emission scanning electron microscopy (FE–SEM) and energy-dispersive X-ray spectroscopy (EDAX) were carried out using SU6600 from Hitachi Ltd. The freeze-fractured surfaces of WPU/ZnO nanocomposites obtained at liquid nitrogen temperature were examined, and all the samples were coated with gold before observation. High-resolution transmission electron microscopy (HRTEM) images and selected area (electron) diffraction (SAED) patterns of ZnO were captured using FEI Technai G^2 (T-30) with an acceleration voltage of 250 kV. The samples for TEM analysis were prepared by dropping dilute suspension of ZnO nanoparticles onto copper grids. Coating thickness was measured using an Elcometer-456 basic c/w for a coating thickness gauge. The surface wettability of the nanocomposite coating was investigated using a water contact angle measurement instrument (Dataphysics OCA35, Data Physics Instruments GmbH, Germany) with the sessile drop method (5.0 μL).

Electrochemical impedance spectroscopy

EIS studies were carried out using a three-electrode cell assembly and an electrochemical analyzer (BAS-IM6) connected to a Thales 4.15 USB software system. A platinum strip with an area of 5 cm^2 served as a counter electrode. A saturated calomel electrode was used as the reference electrode, and the coated MS substrate (area 1 cm^2) served as a working electrode. Studies related to resistance to corrosion were performed at room temperature using a 3.5% aqueous solution of NaCl. Then, 1 cm^2 of the test panel was immersed in the corrosion medium to obtain an open-circuit potential before the start of evaluation. Impedance measurements were recorded using a frequency response analyzer (FRA). The spectrum was recorded in the frequency range of 50 mHz–100 kHz. The applied alternating potential had the root-mean

square amplitude of 10 mV on the E_{OCP}. After recording all the measurements, the system was again allowed to obtain an open-circuit potential. After reaching a stable open-circuit potential, the polarization was carried out using a cathodic potential and an anodic potential which were set at ±200 mV with respect to the corrosion potential at a sweep rate of 1 mV/s. The corrosion potential (E_{corr}) and the corrosion current density (i_{corr}) were deduced from the Tafel plot (log I vs E). The corrosion current was obtained using the Stern–Geary equation:

$$i_{corr} = [b_a b_c / \{2.303(b_a + b_c)\}][1/R_p], \qquad (1)$$

where b_a and b_c are the Tafel slopes or the Tafel constants, expressed in V/decade (V/dec), and R_p is the polarization resistance expressed in kΩ cm^2.

Results and discussion

Surface morphology of ZnO nanoparticles

HRTEM images of ZnO nanoparticles shown in Figs. 1a and 1b clearly depict that the particles are spherical in shape. The sizes of the prepared ZnO nanoparticles fell in the range of 130–145 nm. The morphology of OA-ZnO is similar to that of nano-ZnO (Figs. 1c and 1d). It was confirmed that the long carbon chains and anchoring groups of oleic acid could prevent the aggregation of nanoparticles by spatial steric effect. FE–SEM images also established a proof for the homogeneously dispersed OA-ZnO in the WPU nanocomposite coatings. SAED patterns of nano-ZnO and OA-ZnO shown in Figs. 1a and 1d are in line with the XRD patterns.

Microstructure analysis

The FESEM image of 0.3% OA-ZnO in WPU (Fig. 2 a) nanocomposites clearly indicates the formation of a uniform coating without any defects. Incorporation of OA-ZnO in the WPU matrix effectively sealed the surface by its hydrophobic nature and uniform distribution of nanoparticles in the dispersion. This surface homogeneity has been achieved through good compatibility between the WPU matrix and the ZnO nanoparticles' surface. The surface of the WPU containing 0.3% OA-ZnO after the corrosion resistance test (represented as an FESEM image in Fig. 2b) was found to be slightly rough and uneven. Smoothness of the surface layer was affected, and in a few places, we can observe the minute pits as a result of the corrosion attack. The corrosive media trying to attack the substrate by penetration that causes the damage, however, are not predominant. Figures 2c and 2d show the EDAX spectra of 0.3% OA-ZnO with WPU nanocomposite before and after corrosion studies,
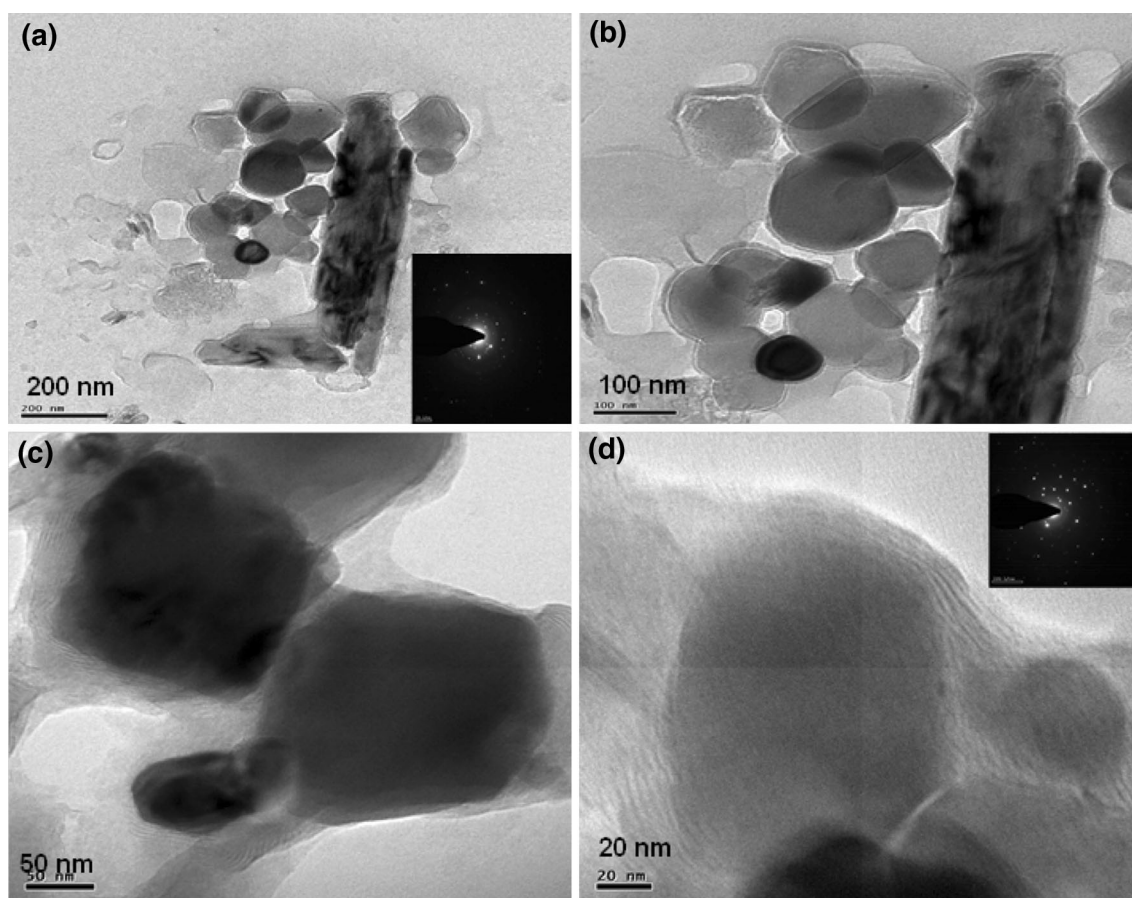
Fig. 1: HRTEM images of ZnO nanoparticles (a) lower magnification (inset with SAED pattern), (b) higher magnification; HRTEM images of OA-ZnO nanoparticles (c) lower magnification, (d) higher magnification (inset with SAED pattern)

which confirmed the presence of zinc and oxygen in the polymer matrix.

XRD patterns

The XRD patterns of ZnO and OA-ZnO nanoparticles are shown in Figs. 3a and 3b. The diffraction peaks corresponding to the (100), (002), (101), (102), (110), (103), and (112) planes are well indexed to the hexagonal phase of ZnO (ICSD Ref. Code-01-076-0704). Both diffractograms showed no changes in the XRD patterns, and the full width at half maximum confirmed that the crystalline structure and the size of ZnO were not affected by surface modification.[33]

Fourier transform infrared (FTIR) spectra

Characterization of ZnO and OA-ZnO nanoparticles

FTIR spectra of nano-ZnO and OA-ZnO are shown in Fig. 4. The peaks located at 2851, 2922, and 473.9 cm^{-1} represent the asymmetric and symmetric stretching vibrations of the $-CH_2$ group and Zn–O stretchings, respectively. The stretching vibration of $O=C-O^-$ in COO–Zn is represented by the peak at $\sim$1545 cm^{-1}. The above results confirm the presence of oleic acid on the surface of ZnO.[33,38]

Characterization of OA-ZnO with WPU nanocomposites

Figure 5(i) shows the FTIR spectra of the various loading levels of OA-ZnO in the as-prepared pure WPU dispersion (PU-687). In addition to all the peaks of the polyurethane (Fig. 5(i) a), in the composite (Figs. 5(i) b–5(i) d), a new peak corresponding to 473.9 cm^{-1} is observed, which is due to the stretching of ZnO (expanded spectrum Fig. 5(ii)). These results suggest that the ZnO is well incorporated into the matrix of the WPU dispersion.[27]

Contact angle measurements

The contact angle of water on the WPU coating was measured as 65.78° (Fig. 6). Films of the said WPU incorporated with OA-ZnO were more hydrophobic,
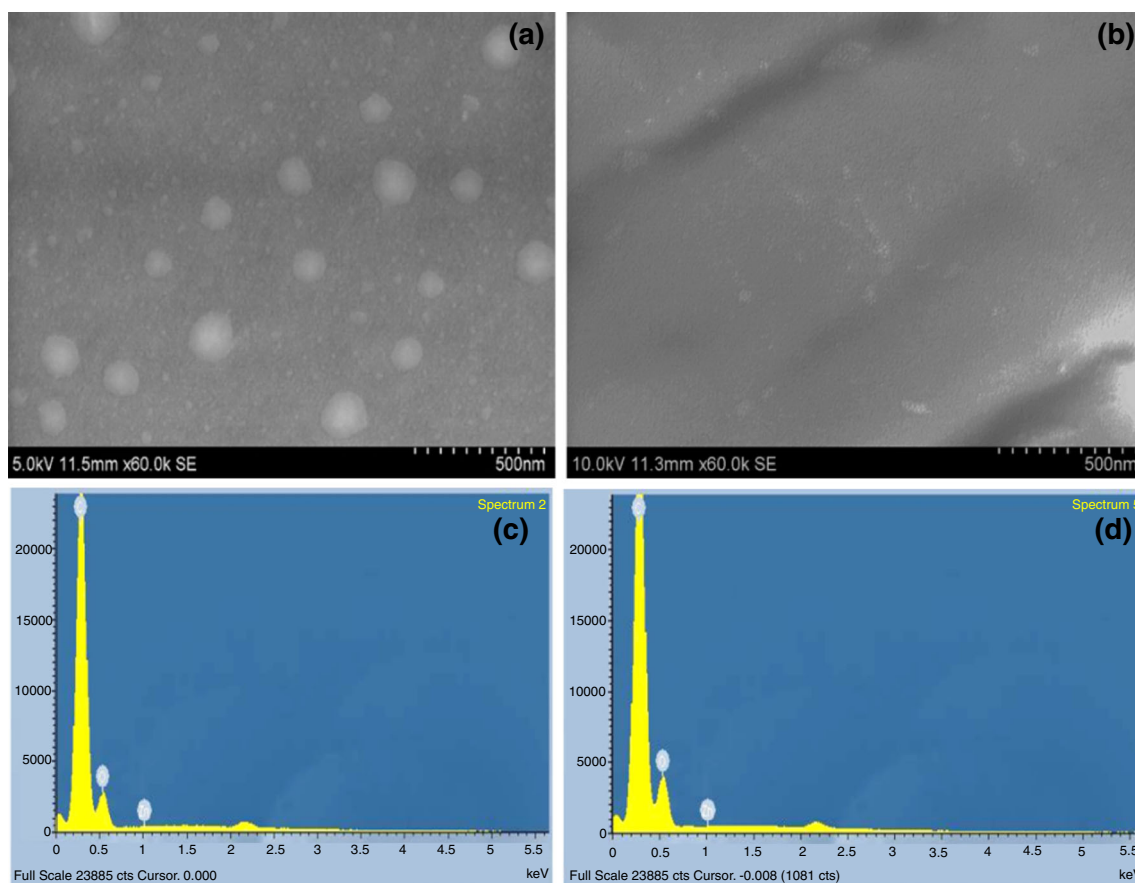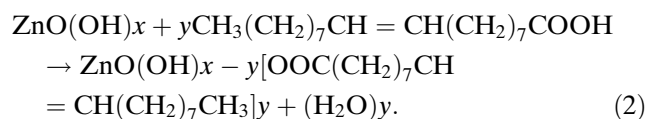
Fig. 2: FESEM images of WPU/0.3% OA-ZnO: (a) before corrosion studies and (b) after corrosion studies and EDAX images of WPU/0.3% OA-ZnO; (c) before corrosion studies and (d) after corrosion studies

which is evident from the increase in the contact angle from 65.78° to 75.87°. The increase in hydrophobicity revealed that the coating is now more resistant to water, whereby the metal surface is prevented from corrosion.

Nanoparticle polymer dispersion

The dispersion of ZnO nanoparticles in the WPU matrix is the key issue in the preparation of WPU/ZnO nanocomposites. Surface active groups in OA could react with ZnO, which decreases its surface energy, and as a result, OA can break up the aggregation, and enhance the dispersion of ZnO in WPU. This surface modification provides nanoparticles free from aggregation due to steric repulsive forces among particles. Moreover, the presence of long alkyl chain and unsaturated bonds in OA on the surface of ZnO provides significant hydrophobicity to the nanoparticles, and this is reflected in the WPU composite coatings (confirmed by contact angle). The WPU dispersion involving OA-ZnO was not settling down (due to homogeneous dispersion) up to a period of 6 months, whereas unmodified nano-ZnO settled down at the bottom within 10 min after ultrasonication (Fig. 7).[23,37]

Therefore, the homogeneous dispersion of ZnO nanoparticles in WPU is confirmed to be significantly enhanced in the presence of OA. The mechanism for surface modification of ZnO is as follows:

$$ZnO(OH)x + yCH_3(CH_2)_7CH = CH(CH_2)_7COOH$$
$$\rightarrow ZnO(OH)x - y[OOC(CH_2)_7CH$$
$$= CH(CH_2)_7CH_3]y + (H_2O)y. \qquad (2)$$

Lipophilic degree of OA-ZnO

The lipophilic degree of prepared ZnO nanoparticles modified by oleic acid were measured by the following method,[33] dispersing 0.5 g of the surface-modified nano-ZnO into 50 mL of water. The unmodified nano-ZnO settled down immediately, while the nano-ZnO coated with oleic acid floated on the water surface. When methanol was added dropwise into the solution slowly under continuous stirring, where the methanol wet the surface of modified ZnO nanoparticles and they precipitated gradually. The volume of methanol used
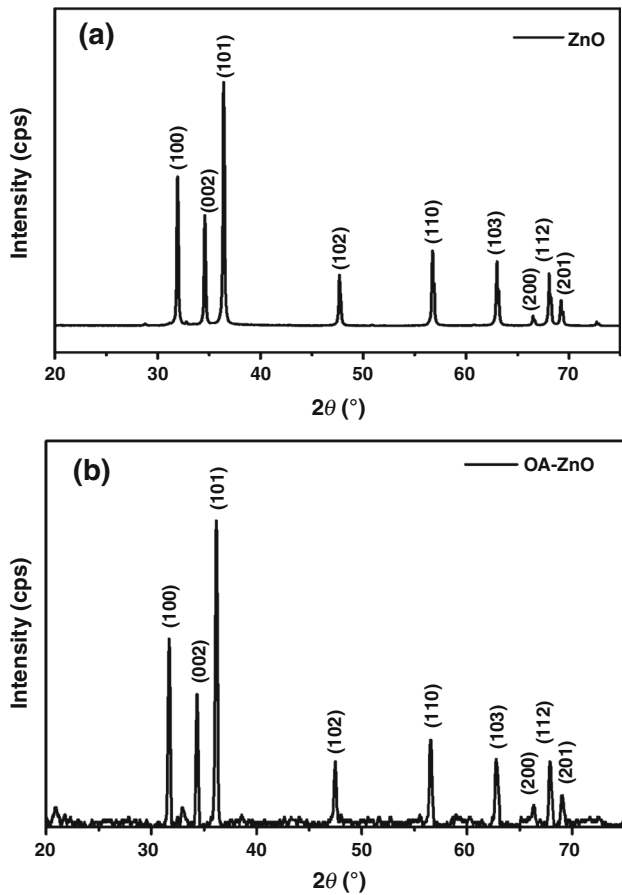
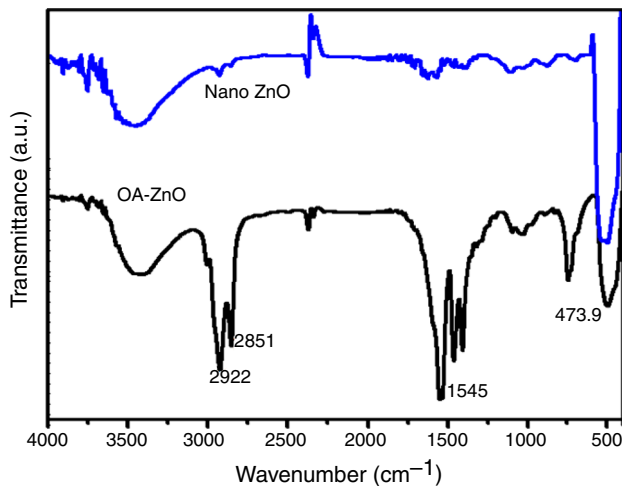Fig. 3: XRD patterns of (a) nano-ZnO and (b) OA-ZnO

Fig. 4: FTIR spectra of nano-ZnO and OA-ZnO

was noted and the lipophilic degree calculated using the following equation (3). The calculated lipophilic degree of surface-modified ZnO was 36%,

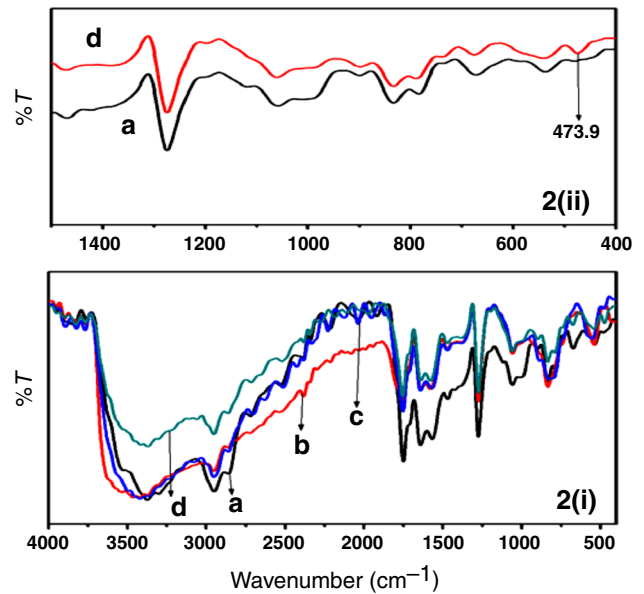$$LD = \{V/(V + 50)\} \times 100\%, \tag{3}$$

Fig. 5: (i) FTIR spectra of (a) WPU, (b) 0.1% of OA-ZnO/WPU nanocomposite, (c) 0.2% of OA-ZnO/WPU nanocomposite, and (d) 0.3% of OA-ZnO/WPU nanocomposite. (ii) Expanded FTIR spectra of (a) WPU and (d) 0.3% of OA-ZnO/WPU nanocomposites

where V is the volume of methanol.

This indicates that the ZnO nanoparticles changed from polarity to nonpolarity after the surface modification by OA.

Electrochemical corrosion studies

Potentiodynamic polarization measurements

The potentiodynamic polarization curves of bare MS and coated MS are shown in Fig. 8. Table 1 summarizes the results determined from the electrochemical curves. The Tafel extrapolation method provides corrosion potential and corrosion current by accurate evaluation from anodic and cathodic Tafel slopes. Corrosion potential (E_{corr}) values of bare MS and MS coated with WPU containing 0.3% OA-ZnO are -0.778 V vs SCE and -0.678 V vs SCE, respectively. This shift toward the positive region confirmed the coated mild steel's increased resistance to corrosion. Also, the decrease in corrosion current density (I_{corr}) from 28.4 to 2.24 $\mu A/cm^2$ and the increase in polarization resistance (R_p) from 0.758 to 13.739 kΩ cm^2 further confirm the enhanced resistance of the coated MS. The shifts in the curves of the Tafel slopes are attributed to various dosages of WPU nanocomposites forming a passive layer coated on the MS surface. This retards both the anodic dissolution of iron and the cathodic hydrogen evolution reaction of the corrosive medium. The coatings inhibit the corrosion that can be
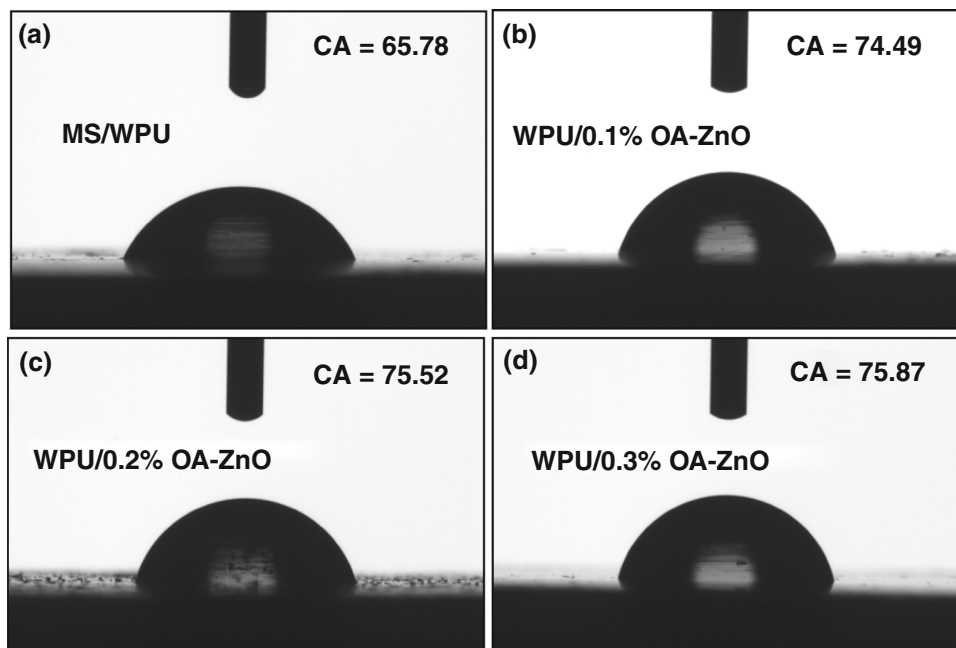
Fig. 6: Contact angles of (a) MS/WPU, (b) WPU/0.1% of OA-ZnO nanocomposite, (c) WPU/0.2% of OA-ZnO nanocomposite, and (d) WPU/0.3% of OA-ZnO nanocomposite
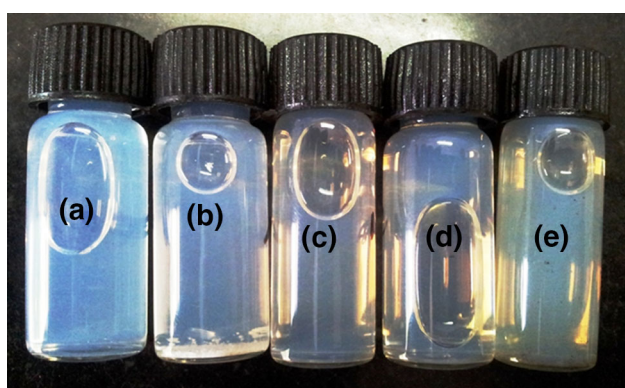

Fig. 7: Stability of dispersions of (a) WPU without nanoparticle, (b) WPU with 0.1% of ZnO nanoparticle, (c) WPU with 0.1% of OA-ZnO nanoparticle, (d) WPU with 0.2% of OA-ZnO nanoparticle, and (e) WPU with 0.3% of OA-ZnO nanoparticle
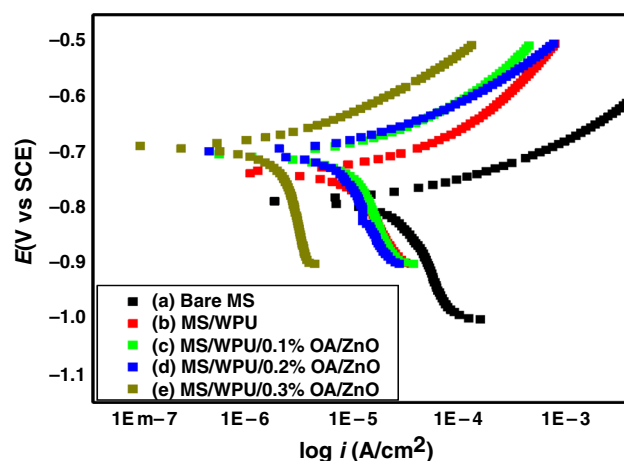

Fig. 8: Potentiodynamic polarization curves of (a) bare MS, (b) MS coated with WPU, (c) MS coated with 0.1% of OA-ZnO WPU nanocomposite, (d) MS coated with 0.2% of OA-ZnO WPU nanocomposite, and (e) MS coated with 0.3% of OA-ZnO WPU nanocomposite

understood through its inhibition efficiency (IE) that is calculated using the formulae given below:

$$\%\text{IE} = \{(I_{corr(0)} - I_{corr(i)})/I_{corr(0)}\} * 100, \qquad (4)$$

$$\%\text{IE} = \{(R_{ct(i)} - R_{ct(0)})/R_{ct(i)}\} * 100, \qquad (5)$$

where $I_{corr(0)}$ is the corrosion current density of bare MS, and $I_{corr(i)}$ is the corrosion current density of the WPU nanocomposite-coated MS. $R_{ct(0)}$ is the charge transfer resistance of bare MS, and $R_{ct(i)}$ is the charge transfer resistance of WPU nanocomposite-coated MS. The calculated %IE values are shown in Tables 1 and 2. Also, the other parameters measured from the values from Tafel curves of the prepared coatings were porosity and corrosion rate.

Both are calculated using the following relationship:

$$\%P = (R_{pol}/R_{pol}^*)\left(10^{-(\Delta E_{corr}/b_a)}\right) \times 100 \qquad (6)$$

Table 1: Potentiodynamic polarization data of MS and MS coated with different WPU nanocomposites in 3.5% NaCl solution

Sample	I_{corr} ($\mu A/cm^2$)	E_{corr} (V)	b_a (V/dec)	b_c (V/dec)	R_p ($k\Omega\ cm^2$)	I_{corr} %IE	P %	CR (mm/year)
MS	28.40	−0.778	0.056	−0.435	0.75	−		0.33
MS/WPU	10.50	−0.739	0.076	−0.486	2.72	63.02	5.58	0.12
MS/WPU/0.1% OA-ZnO	9.76	−0.698	0.068	−0.304	2.47	65.63	1.13	0.11
MS/WPU/0.2% OA-ZnO	6.01	−0.692	0.060	−0.282	3.57	78.83	0.61	0.07
MS/WPU/0.3% OA-ZnO	2.24	−0.678	0.078	−0.776	13.74	92.11	0.08	0.02

MS mild steel, *WPU* waterborne polyurethane, *OA-ZnO* nano-ZnO surface modified with oleic acid

Table 2: Impedance data obtained by equivalent circuits of MS and MS coated with different WPU nanocomposite coatings studied in the present work

Sample	R_s ($\Omega\ cm^2$)	$Q_{coat} - y_o$ ($\mu F/cm^2$)	n_c	R_{pore} ($\Omega\ cm^2$)	$Q_{dl} - y_o$ ($\mu F/cm^2$)	n_{dl}	R_{ct} ($\Omega\ cm^2$)	R_{ct} IE%
MS	8.59	−	−	−	364.4	0.87	196.82	−
MS/WPU	9.95	426.02	0.78	137.26	236.08	0.85	491.07	59.92
MS/WPU/0.1% OA-ZnO	12.83	310.01	0.75	165.91	162.4	0.78	650.43	69.74
MS/WPU/0.2% OA-ZnO	18.43	238.63	0.72	198.73	121.01	0.77	1482	86.71
MS/WPU/0.3% OA-ZnO	26.87	119.52	0.69	347.01	71.5	0.72	3056	93.55

MS mild steel, *WPU* waterborne polyurethane, *OA-ZnO* nano-ZnO surface modified with oleic acid

where P is the total porosity, R_{pol} and R_{pol}^* are the polarization resistances of bare and coated mild steel, ΔE_{corr} is the corrosion potentials differences of bare and coated mild steels, and b_a is the anodic Tafel slope for bare mild steel.

$$\text{Corrosion rate (CR)} = K_1 \times (I_{corr}/\rho) \times EW, \qquad (7)$$

where $K_1 = 3.27 \times 10^{-3}$ (mm g/μA cm year), I_{corr} = corrosion current density, ρ = density in g/cm^3, EW is the equivalent weight for mild steel (EW is dimensionless in this calculation), and CR is given in mm/year. The equivalent weight of the MS is estimated to be 28.25.

The porosity values of the coatings determine their ability to protect the substrate against corrosion. The calculated porosity values for coatings are given in Table 1. The porosity values of the WPU nanocomposites decrease in the following order: MS/WPU > MS/WPU/0.1% OA-ZnO > MS/WPU/0.2% OA-ZnO > MS/WPU/0.3% OA-ZnO (while the increase in the dosages of nano-ZnO by this blending method was not able to allow dispersing the particles without disturbing the polymer matrix during the short time of sonication). So the 0.3% OA-ZnO/WPU nanocomposite coating on MS was found to be a compact coating, with porosity values almost 63, 12, and 6 times lower than those in MS/WPU, MS/WPU/0.1% OA-ZnO, MS/WPU/0.2% OA-ZnO. Moreover, corrosion rates of MS/WPU/0.3% OA-ZnO almost 13 times lower than the calculated values of the bare MS are given in Table 1. The above results confirmed that, as the dosage of OA-ZnO increases, the

hydrophobicity of the coating increases, which disallows water penetration into the substrate, thereby increasing the resistance to corrosion.

Impedance measurements

The effect of NaCl solution (3.5% in water) on the bare MS and MS coated with WPU nanocomposite was studied by EIS at room temperature after 1 h of immersion; the difference in corrosion resistances was understood from Nyquist curves shown in Fig. 9, and their equivalent circuits are represented as $R(QR)$ and $R(Q[R(QR)])$ in Fig. 10. The proposed equivalent circuit for a mild-steel substrate is shown in Fig. 10a, which is the equivalent circuit model for a simple corrosion system. This system is completely charge transfer controlled. Polarity and the amount of charge at the substrate/electrolyte interface were provided by double-layer capacitance. This circuit shows a working electrode (WE), solution resistance (R_s), charge transfer resistance (R_{ct}), and double-layer capacitance (Q_{dl}). Here the double-layer capacitance represents the substrate/electrolyte interface, and Q stands for constant phase element (CPE) for better quality fit to the proposed system. This equation is written as

$$Y(\omega) = Y_0(j\omega)^n \qquad (8)$$

where Y_0 is used in the nonlinear least squares fitting, and n is the CPE exponent which always lies in
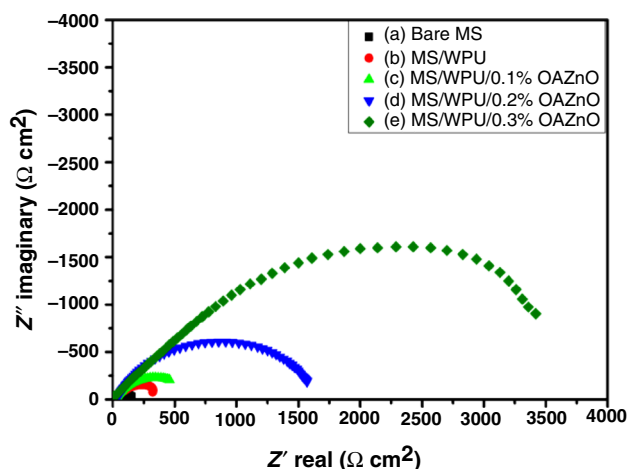
Fig. 9: Nyquist plots of (a) bare MS, (b) MS coated with WPU, (c) MS coated with 0.1% of OA-ZnO/WPU nanocomposite, (d) MS coated with 0.2% of OA-ZnO/WPU nanocomposite, and (e) MS coated with 0.3% of OA-ZnO/WPU nanocomposite
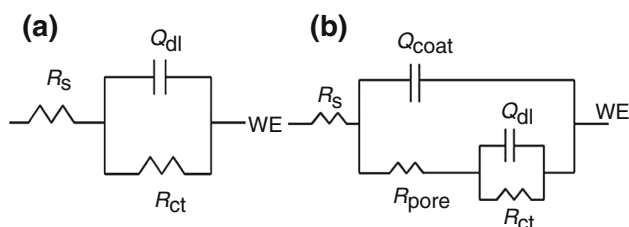

Fig. 10: (a) Equivalent circuits for the EIS data of the mild steel substrate and (b) equivalent circuits used for fitting the EIS data of mild steel and mild steel coated with different WPU nanocomposites

between 0 and 1. Both are adjustable parameters. CPE can be considered as a real capacitance when $n = 1$ and real resistance when $n = 0$, and ω is the angular frequency (in rad s^{-1}).

The circuit description code (CDC) for the equivalent circuit for the mild steel substrate is $R(QR)$. The equivalent circuit for WPU nanocomposites coated on MS substrate is shown in Fig. 10b. Coated substrate was introduced into the electrolyte solution where the defect in the coating provide the direct diffusion path for the corrosive media. Thus, localized corrosion dominates in the corrosion process. This coated substrate can be divided into two sub-interfaces: electrolyte/coating and electrolyte/substrate. This circuit consists of the equivalent circuits R_{pore} and Q_{coat}, which are related to electrolyte/coating interface reactions. R_{ct} and Q_{dl} are related to the charge-transfer reactions at the electrolyte/substrate interface. The CDC of the proposed equivalent circuit for the coated sample is $R(Q[R(QR)])$.

The increase in charge-transfer resistance (R_{ct}) from 196.82 to 3056 Ω cm^2 (Table 2) further explains that

the MS coated with WPU nanocomposites are corrosion resistant. Corrosion resistance was found to increase with the increasing dosage of OA-ZnO. The above result implies that the WPU nanocomposite coatings are more inert toward the electrochemical corrosion. This is due to more crosslinked structures of WPU with the increasing OA-ZnO content, which prevent the penetration of corrosive species by acting as a strong physical barrier. This was also explained by contact angle values; increasing the dosage of OA-ZnO in the coating, which increases the hydrophobicity of the coating, also reduces the diffuse pathways of corrosive species into the coating and increases the corrosion resistance of the WPU nanocomposite coatings.
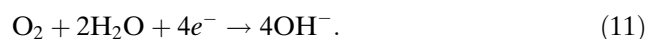
Mechanism of WPU nanocomposite coatings

According to the electrochemical theory, corrosion can be defined as degradation of a material due to one anodic (oxidation of metals) and one cathodic (reduction of dissolved oxygen) reaction. The mechanism of galvanic interactions on the metal surfaces is the same as that in neutral environmental conditions. The metal ions release electrons from their surfaces and they get dissolved as ions in solution. The ions flow through the metal by means of the electrolyte and get reduced at cathode.

Oxidation of metal at anode

$$Fe \rightarrow Fe^{2+} + 2e^- \tag{9}$$

$$2Fe^{2+} \rightarrow 2Fe^{3+} + 2e^- \tag{10}$$

Reduction of oxygen at cathode

$$O_2 + 2H_2O + 4e^- \rightarrow 4OH^-. \tag{11}$$

The strong interaction of hydrophobically modified nano-ZnO in the WPU are dispersed uniformly throughout the coatings, and this could be attributed to the fact that the greater surface activity of nanoparticles absorbs more resin on its surface, which enhances the density of the coating, thereby preventing corrosion. ZnO acts as a barrier filler to seal pores in the coatings and improve the barrier protection.

So the following reaction can be retarded

$$2Fe_{(aq)}^{2+} + O_{2(g)} + 2H_2O \rightarrow 2FeOOH + 2H^+. \tag{12}$$
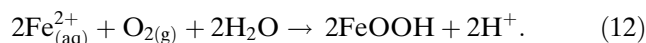
Herein, we have concluded that the protection mechanism (Scheme 1) is based on two pathways: In the presence of ZnO nanoparticles, Zn is converted into Zn^{2+} acting as a cation ion, and it can easily passivate the substrate. Even small percentages of these cations are able to inhibit the corrosion of the substrate. This mechanism is attributed to block the free iron surface for the cathodic complementary

(I)

(II)
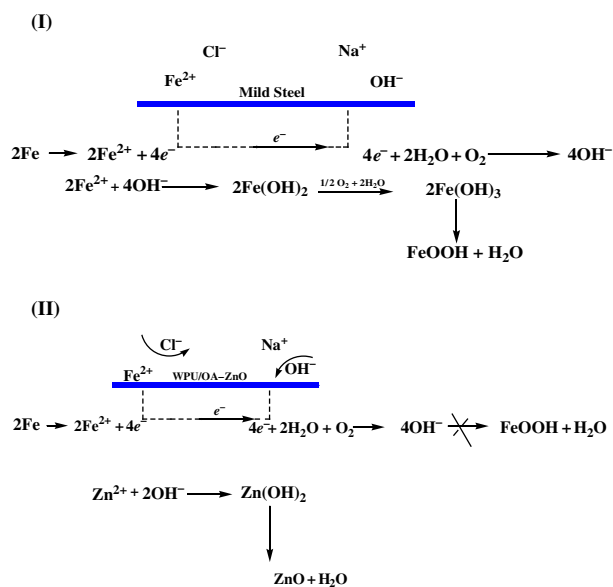
Scheme 1: Mechanism for corrosion protection using WPU nanocomposites coatings. (I) Formation of corrosion product on mild steel. (II) Protection of mild steel from corrosion

hydrogen evolution reaction and increase the resistance to corrosion. There is another way to explain this mechanism: filling the pores of the coating by surface-modified nano-ZnO would prevent the mobility of corrosive species to the substrate. This can act as barrier protection filler.[14,40] Among the investigated coatings, the Q_{coat} and Q_{dl} values decreased and R_s and R_{ct} values increased in the one with 0.3% OA-ZnO composite compared with the (bare) mild steel substrate, indicating that the increasing concentration of OA-ZnO into the waterborne dispersion could improve the resistance to corrosion.

Conclusion

The present work describes the role of surface-modified nanoparticles in improving the corrosion resistance of MS. The results of the study revealed that the surface-modified nano-ZnO was more stable than the unmodified ZnO in the dispersion. The modified ZnO nanoparticles are dispersed uniformly throughout the WPU coating, to prevent the mobility of corrosive species to the substrate, thereby preventing corrosion. Potentiodynamic polarization and EIS measurements confirmed that MS coated with WPU containing 0.3% OA-ZnO nanocomposite showed improved resistance to corrosion. In the future, more studies are needed to enhance the protection efficiencies of the nanoparticles and their interfacial interactions with polymer matrix, by simpler blending method with facile processing ability, and to minimize the time

and cost of engineering in the coatings industry by improving the surface characteristics of the polymer, like hydrophobicity and barrier protection efficiency with incorporation of lower dosage of the surface-modified nanoparticles.

References

1. Shi, X, Nguyen, TA, Suo, Z, Liu, Y, Avci, R, "Effect of Nanoparticles on the Anticorrosion and Mechanical Properties of Epoxy Coating." *Surf. Coat. Technol.*, **204** 237–245 (2009)
2. Frau, AF, Pernites, RB, Advincula, RC, "A Conjugated Polymer Network Approach to Anticorrosion Coatings: Poly (vinylcarbazole) Electrodeposition." *Ind. Eng. Chem. Res.*, **49** 9789–9797 (2010)
3. Kuang, W, Mathews, JA, Taylor, ML, Macdonald, DD, "The Effect of Anodamine on the Corrosion Behavior of 1018 Mild Steel in Deionized Water: II. Electrochemical Impedance Analysis." *Electrochim. Acta*, **136** 493–503 (2014)
4. Dhoke, SK, Khanna, AS, "Electrochemical Impedance Spectroscopy (EIS) Study of Nano-alumina Modified Alkyd Based Waterborne Coatings." *Prog. Org. Coat.*, **74** 92–99 (2012)
5. Vengatesh, P, Anbu Kulandainathan, M, "Hierarchically Ordered Self-Lubricating Superhydrophobic Anodized Aluminum Surfaces with Enhanced Corrosion Resistance." *Appl. Mater. Interfaces*, **7** 1516–1526 (2015)
6. Ramezanzadeh, B, Attar, MM, "Studying the Corrosion Resistance and Hydrolytic Degradation of an Epoxy Coating Containing ZnO Nanoparticles." *Mater. Chem. Phys.*, **130** 1208–1219 (2011)
7. Rahman, OU, Kashif, M, Ahmad, S, "Nanoferrite Dispersed Waterborne Epoxy-Acrylate: Anticorrosive Nanocomposite Coatings." *Prog. Org. Coat.*, **80** 77–86 (2015)
8. Sørensen, PA, Kiil, S, Johansen, KD, Weinell, CE, "Anticorrosive Coatings: A Review." *J. Coat. Technol. Res.*, **6** 135–176 (2009)
9. Olad, A, Naseri, B, "Preparation, Characterization and Anticorrosive Properties of a Novel Polyaniline/Clinoptilolite Nanocomposite." *Prog. Org. Coat.*, **67** 233–238 (2010)
10. Dhoke, SK, Khanna, AS, Sinha, TJ, "Effect of Nano-ZnO Particles on the Corrosion Behavior of Alkyd-Based Waterborne Coatings." *Prog. Org. Coat.*, **64** 371–382 (2009)
11. Liang, LH, Mei, K, Gu, L, Wang, SS, "Corrosion Protection of Mild Steel by Zirconia Sol-Gel Coatings." *J. Mater. Sci. Lett.*, **20** 1081–1083 (2001)
12. Chen, Y, Zhou, S, Yang, H, Wu, L, "Structure and Properties of Polyurethane/Nanosilica Composites." *J. Appl. Polym. Sci.*, **95** 1032–1039 (2005)
13. Yue-Jian, C, Juan, T, Fei, X, Jia-Bi, Z, Ning, G, Yi-Hua, Z, Ye, D, Liang, G, "Synthesis, Self-assembly, and Characterization of PEG-Coated Iron Oxide Nanoparticles as Potential MRI Contrast Agent." *Drug Dev. Ind. Pharm.*, **36** 1235–1244 (2010)

14. Mostafaei, A, Nasirpouri, F, "Electrochemical Study of Epoxy Coating Containing Novel Conducting Nanocomposite Comprising Polyaniline–ZnO Nanorods on Low Carbon Steel." *Corr. Eng. Sci. Technol.*, **48** 513–524 (2013)

15. Jeeva Jothi, K, Palanivelu, K, "Facile Fabrication of Core-Shell Pr6O11-ZnO Modified Silane Coatings for Anticorrosion Applications." *Appl. Surf. Sci.*, **288** 60–68 (2014)

16. Olad, A, Nosrati, R, "Preparation and Corrosion Resistance of Nanostructured PVC/ZnO Polyaniline Hybrid Coating." *Prog. Org. Coat.*, **76** 113–118 (2013)

17. Qing, Y, Yang, C, Hu, C, Zheng, Y, Liu, C, "A Facile Method to Prepare Superhydrophobic Fluorinated Polysiloxane/ZnO Nanocomposite Coatings with Corrosion Resistance." *Appl. Surf. Sci.*, **326** 48–54 (2015)

18. Hang, TTX, Dung, NT, Truc, TA, Duong, NT, Truoc, BV, Vu, PG, Hoang, T, Thanh, DTM, Olivier, MG, "Effect of Silane Modified Nano ZnO on UV Degradation of Polyurethane Coatings." *Prog. Org. Coat.*, **79** 68–74 (2015)

19. Nicolay, A, Lanzutti, A, Poelmanc, M, Ruellec, B, Fedrizzi, L, Dubois, P, Olivier, MG, "Elaboration and Characterization of a Multifunctional Silane/ZnO Hybrid Nanocomposites." *Appl. Surf. Sci.*, **327** 379–388 (2015)

20. Shen, GX, Chen, YC, Lin, L, Lin, CJ, Bury, DS, "Study on a Hydrophobic Nano-TiO$_2$ Coating and Its Properties for Corrosion Protection of Metals." *Electrochim. Acta*, **5** 5083–5089 (2005)

21. Kango, S, Kalia, S, Celli, A, Njuguna, J, Habibi, Y, Kumar, R, "Surface Modification of Inorganic Nanoparticles for Development of Organic-Inorganic Nanocomposites—A Review." *Prog. Polym. Sci.*, **38** 1232–1261 (2013)

22. Zeng, Z, Yu, J, Guo, ZX, "Preparation of Functionalized Core-Shell Alumina/Polystyrene Composite Nanoparticles, Encapsulation of Alumina Via Emulsion Polymerization." *Macromol. Chem. Phys.*, **206** 1558–1567 (2005)

23. Gao, X, Zhou, B, Guo, Y, Zhu, Y, Chen, X, Zheng, Y, Gao, W, Ma, X, Wang, Z, "Synthesis and Characterization of Well-Dispersed Polyurethane/CaCO$_3$ Nanocomposites." *Colloids Surf. A*, **371** 1–7 (2010)

24. Chen, J, Zhou, Y, Nan, Q, Sun, Y, Ye, X, Wang, Z, "Synthesis, Characterization and Infrared Emissivity Study of Polyurethane/TiO$_2$ Nanocomposites." *Appl. Surf. Sci.*, **253** 9154–9158 (2007)

25. Gao, X, Zhu, Y, Zhao, X, Wang, Z, An, D, Ma, Y, Guan, S, Du, Y, Zhou, B, "Synthesis and Characterization of Polyurethane/SiO$_2$ Nanocomposites." *Appl. Surf. Sci.*, **257** 4719–4724 (2011)

26. Zhu, A, Cai, A, Yu, Z, Zhou, W, "Film Characterization of Poly(styrene-butylacrylate-acrylic acid)–Silica Nanocomposites." *J. Colloid Interface Sci.*, **322** 51–58 (2008)

27. Mishra, AK, Mishra, RS, Narayan, R, Raju, KVSN, "Effect of Nano ZnO on the Phase Mixing of Polyurethane Hybrid Dispersions." *Prog. Org. Coat.*, **67** 405–413 (2010)

28. Hong, RY, Chen, LL, Li, JH, Li, HZ, Zheng, Y, Ding, J, "Preparation and Application of Polystyrene-Grafted ZnO Nanoparticles." *Polym. Adv. Technol.*, **18** 901–909 (2007)

29. Mahdavian, AR, Sarrafi, Y, Shabankareh, M, "Nanocomposite Particles with Core-Shellmorphology III: Preparation and Characterization of Nano Al$_2$O$_3$–Poly(styrene–methyl methacrylate) Particles via Miniemulsion Polymerization." *Polym. Bull.*, **63** 329–340 (2009)

30. Saleema, N, Farzaneh, M, "Thermal Effect on Superhydrophobic Performance of Stearic Acid Modified ZnO Nanotowers." *Appl. Surf. Sci.*, **254** 2690–2695 (2008)

31. Tang, E, Dong, S, "Preparation of Styrene Polymer/ZnO Nanocomposites Latex via Miniemulsion Polymerization and Its Antibacterial Property." *Colloid Polym. Sci.*, **287** 1025–1032 (2009)

32. Li, Z, Zhu, Y, "Surface-Modification of SiO$_2$ Nanoparticles with Oleic Acid." *Appl. Surf. Sci.*, **211** 315–320 (2003)

33. Hong, R, Pan, T, Qian, J, Li, H, "Synthesis and Surface Modification of ZnO Nanoparticles." *Chem. Eng. J.*, **119** 71–81 (2006)

34. Mahdavian, A, Ashjari, M, Makoo, AB, "Preparation of Poly(styrene–methylmethacrylate)/SiO$_2$ Composite Nanoparticles via Emulsion Polymerization. An Investigation into the Compatibilization." *Eur. Polym. J.*, **43** 336–344 (2007)

35. Liu, P, "Facile Preparation of Monodispersed Core/Shell Zincoxide@polystyrene (ZnO@PS) Nanoparticles via Soapless Seeded Microemulsion Polymerization." *Colloids Surf. A*, **29** 155–161 (2006)

36. Liu, D, Wu, W, Qiu, Y, Yang, S, Xiao, S, Wang, Q, Ding, L, Wang, J, "Surface Functionalization of ZnO Nanotetrapods with Photoactive and Electroactive Organic Monolayers." *Langmuir*, **24** 5052–5059 (2008)

37. Gao, X, Zhu, Y, Zhou, S, Gao, W, Wang, Z, Zhou, B, "Preparation and Characterization of Well-Dispersed Waterborne Polyurethane/CaCO$_3$ Nanocomposites." *Colloids Surf. A*, **377** 312–317 (2011)

38. Augustinen, MS, Jeeju, PP, Sreevalsa, VG, Jayalekshmi, S, "Excellent UV Absorption in Spin-Coated Thin Films of Oleic Acid Modified Zinc Oxide Nanorods Embedded in Polyvinyl Alcohol." *J. Phys. Chem. Solids*, **73** 396–401 (2012)

39. Mahmoudian, MR, Basirun, WJ, Alias, Y, Zak, AK, "Electrochemical Characteristics of Coated Steel with Poly(N-methyl pyrrole) Synthesized in Presence of ZnO Nanoparticles." *Thin Solid Films*, **520** 258–265 (2011)

40. Sonawane, SH, Teo, BM, Brotchie, A, Grieser, F, Ashokkumar, M, "Sonochemical Synthesis of ZnO Encapsulated Functional Nanolatex and Its Anticorrosive Performance." *Ind. Eng. Chem. Res.*, **49** 2200–2205 (2010)